IEEE Access
Multidisciplinary | Rapid Review | Open Access Journal

Received April 25, 2019, accepted May 30, 2019, date of publication June 13, 2019, date of current version June 27, 2019.

Digital Object Identifier 10.1109/ACCESS.2019.2922242

Wear Analysis of Tube-Baffle Vibration Interaction in a Tube Bundle

MUHAMMAD USMAN[1, 2], SHAHAB KHUSHNOOD[1], LUQMAN AHMAD NIZAM[1], MUHAMMAD AYUB[2], AKMAL HAFEEZ[1], BEHZAD RUSTAM[2], JUNAID MUHAMMAD YOUSUF[2], AND MUHAMMAD SHAHID BASHIR[1]

[1]Department of Mechanical and Aeronautical Engineering, University of Engineering and Technology, Taxila 47050, Pakistan
[2]Department of Mechanical Engineering, The University of Lahore, Lahore 54000, Pakistan

Corresponding author: Muhammad Usman (muhammadusman3051@gmail.com)

ABSTRACT Wear analysis has been carried out on aluminum tube in parallel triangular tube bundle with P/D ratio of 1.45 and the baffle plate placed at the mid-span of the bundle. The cross-flow velocity of water ranges from 0.18 m/s to 0.55 m/s. For each flow velocity, tests were performed on five different flow velocities and three-time spans (tube-baffle interaction) i.e., 30, 60, and 90 min. The experiments were designed in a unique way to study the relationship between cross flow velocity and tube baffle interaction time with wear produced on the tube surface. This is the first study of its kind in which wear analysis of a flexible tube has been done in the water tunnel to simulate the real environment of the heat exchanger tubes. The vibration response of the monitored tube was acquired using a tri-axial wireless accelerometer. A Scanning Electron Microscope (SEM) was used for the measurement of wear sizes. It was observed that the transverse amplitude rises significantly at higher velocities as compared to streamwise amplitude results in significant wear in the transverse direction. The wear sizes also tend to increase with the cross-flow velocity and become prominent at higher velocities. A similar trend has been observed for the wear area and wears volume. Also with the increase in the tube-baffle interaction span, the wear scar tends to be deeper and wider significantly at higher velocities.

INDEX TERMS Flow-induced vibrations, fretting wear, parallel triangular, wear scar.

I. INTRODUCTION

Heat exchangers are one of the most important components of process and petrochemical industries and are thus part of ongoing research for the past five decades to improve their design and increase their performance. Shell and tube type heat exchangers are the most common form of heat exchangers used in industries. Shell and tube type heat exchangers generally have baffles that provide support to tubes and increase structural rigidity and thermal efficiency as well as in some cases direct the flow. Flow-induced vibrations in heat exchangers cause tube-to-support interaction. This interaction causes the failure of the heat exchanger tube bundle due to wear.

Heat exchanger tube bundles are composed of generally thin and long tubes supported at the end. As the tubes have a low slenderness ratio, the supports provide structural rigidity and stability to the tubes.

During the operation, a tube bundle goes under a complex system of forces that produces vibrations in the tubes. Fluid flow is responsible for making vibration and noise problems that hinder the smooth running of the plant operation. Vibrations that arise because of fluid flow are called ''Flow-Induced Vibrations'' (FIV). It has been established that forces in a fluid may vary due to a number of reasons and when an obstacle is placed in their path, they may cause its vibrations. During vibration, slippage occurs between the tube and the support contact. A slip can cause tubes to be worn out which may lead to failure. For example, a leakage in the fuel tubes in a heat exchanger caused by wear can lead to the release of dangerous gases in the fluid flow. Wear causes thinning of tubes which results in loss of structural integrity which ultimately causes loss of power control. It is thus always recommended to control the wear rate of the tubes. Theoretically, such wear can be removed by moving the support with the

The associate editor coordinating the review of this manuscript and approving it for publication was Jiafu Wan.

tube, however, the design conditions restrict doing so. During heat exchanger operation the tubes being made of metal, grow according to its coefficient of thermal expansion because of high temperature and irradiation effect in the exchanger. The tube contacts are supposed to have a considerable allowance to compensate for the growth of tubes, so generally, a small gap is employed or a contact force less than which prevents the tubes from growing. Wear is often more characteristic, severe and detrimental in the presence of a gap as found in research [1]. A sliding and impact mechanism instead of only a sliding mechanism was considered and investigated to explain elevated wear rates when a gap was present. Steam generator heat exchanger tubes wear show a flow induced fretting wear problem. There are several wear mechanisms and it is found that usually more than one wear mechanism is involved in particular wear. Still, adhesion and abrasion could be regarded as primary fretting wear. Adhesion initiates fretting wear and abrasion occurs once the particles are oxidized [2]. Particle dispersion has a considerable effect on the fretting wear rate. Since 1970's Blevins and other researchers have started exploring the wear phenomenon in tube bundle of the heat exchanger and steam generators. Their research has resulted in valuable information about understanding wear mechanisms.

An important aspect for engineers and designers is to estimate the overall life of a structure. Meng and Ludema [3] have summarized the existing wear models. It has been found through literature that weight loss, wear of depth and volume are the three most important parameters for wear study as these parameters determine the severity of the wear. During the nuclear component modeling, one of these parameters i.e. wear volume parameter is used that led to the development of ''work rate model'' which in turn is used to find out the wear in the tubes that are used in nuclear steam generator [4] and nuclear fuel tubes [5]. This is given as Eq. (1)

$$\dot{V} = K\dot{W} \tag{1}$$

where, $\dot{V}$ is the time rate of increase of wear volume and $\dot{W}$ is the rate of work and K is termed as the coefficient of wear and its dimension is Pa^{-1}. However, tube thickness reduction is directly linked with the rigidity of the structure and fuel integrity is steam generators. Therefore, the depth of wear can be regarded as a more critical parameter as compared to wear volume. The wear depth instead of wear volume can be regarded as a more critical parameter since the perforation of the tubes as well as the structural rigidity and integrity of the fuel or steam generator tubes is directly related with the reduction in thickness of the tubes. The maximum wear depth is likely to be localized arbitrarily as the collision of each tube is slightly different than the rest of the tubes in the bundle based on their location thus making it difficult to determine the maximum depth easily [6]. The arbitrariness of the maximum depth location can also be explained if considered a locally different wear mechanism. A development of parameter that can define the degree of wear accurately and with appropriate severity is the current need, so that cases where thickness reduction is of particular concern can be dealt with accordingly.

Components of a cross-flow heat exchanger include a baffle placed along the tubes which makes the tubes flexible. Generally in heat exchanger designing, when the size of the heat exchanger is increased, the fluid velocity on the shell side also increases because of which the heat transfer rate increases. Therefore, clearance in the tube bundle baffles is kept for the expansion of the tubes during the process. That clearance produces flow-induced vibration in the tube bundle with high amplitude past a critical velocity of fluid flow. Due to these problems fretting wear and necking type failures occur in the tube bundle. The earlier studies on fretting wear by Connors [7], Blevins [8] and Ko [9] predicts interesting results. The study by Connors provided a formula for wear scars of pyramidal and crescent shapes, but some other shapes like oblique and flat wear scars were not part of his research. Au-Yang [10] carried out research on tubes used in the steam generator and observed the phenomena of flow-induced wear, and a comparison was made between his results and actual operations. He considered the effects caused by the gap between the tubes. By calculating the time rate of depletion of the thickness of the tube wall, he concluded that the fluid elastic force is also responsible for the wear phenomena along with turbulence excitation. Fretting wear caused by turbulence excitation in heat exchanger tube bundle was studied by Yetisir et al. [11] and a work rate criteria were presented in this study to calculate this damage. [12] carried out research on heat exchanger tubes and calculated wear between two mating components because of the interactions between the tubes and support plate.

II. WEAR MODELS

A number of wear models related to tube bundles have been proposed by researchers. Each wear model has its own assumptions and conditions. Therefore, no general model of wear is readily available. Archard [13] in 1953 published a wear model mainly considering of adhesive wear phenomenon that can be presented in its simplest form as Eq. (2).

$$V = K\left(\frac{P}{H}\right)L \tag{2}$$

where V is wear volume, P is a normal force on the surface, L is sliding distance, H is material hardness and K is wear coefficient (10^{-1} *to* 10^{-10}). This model has dominated on both theoretical and experimental analysis of wear phenomenon and is widely studied. The Archard model originally for adhesive wear was later intended to both wear mechanism analysis such as abrasion fatigue wear and corrosion. Normally at the location of the tube supported with baffles, the wear occurs due to the fretting contact between the outer side of the tube and inner side of the baffle hole. It is generally expected that the round wear scar should produce on the tube surface at the support location. In this case,

the wear depth (h) can be calculated from Eq. (3) [14]

$$h = \frac{d - \sqrt{d^2 - \frac{4V}{\pi w}}}{2} \tag{3}$$

where V is wear volume, d is the diameter of the tube and w is the width of the baffle plate. In case of round wear scar, the wear depth has an almost linear relationship with the wear volume. The main reason for this kind of wear scar is due to the orbited motion of tube at support plate. Jain and Bahadur [15] developed a sliding wear model of polymeric materials based on fatigue and topography of the sliding surface. The model has two assumptions.

- The deformation in the contact zone is mainly of an elastic nature.
- Both the sliding surfaces have roughness.

There are basically four equations to demonstrate the model. Firstly the real contact is determined by Hertzian equation for each individual asperity. The Hertzian equations for the elastic contact provided as Eq. (4-7)[15].

$$\mathrm{a}_1 = \sqrt{\beta\omega} \tag{4}$$

$$A_1 = \pi\beta\omega \tag{5}$$

$$P_1 = \frac{4}{3}E'\sqrt{\beta\omega} \tag{6}$$

$$\frac{1}{E'} = \frac{1-\gamma_1^2}{E_1} + \frac{1-\gamma_2^2}{E_2} \tag{7}$$

where γ is poison's ratio, ω is the compliance, β is the radius of spherical asperity, E is elastic modulus and P_1 is the normal load. Greenwood and Williamson [16] extended the above single contact equations to the case of contact between a rough and a smooth surface. By normalizing with respect to the standard deviation of the asperity height distribution, the equations are presented in Eq. (8-10).

$$n_\circ = \eta A_0 F_0(h) \tag{8}$$

$$A_r = \pi\eta A_0 \beta\sigma F_1(h) \tag{9}$$

$$P = \frac{4}{3}\eta A_0 E\sqrt{\beta}\sigma^{\frac{3}{2}} F^{\frac{3}{2}}(h) \tag{10}$$

where, $n_\circ$ is discrete contact zones, A_r is the area of real contact, P is load, η is the surface density of asperities, A_0 is the nominal area of contact and σ is the standard deviation of the asperity height distribution. The generalized function $F_n(h)$ is defined as Eq. (11)

$$F_n(h) = \int_h^\infty (\mathrm{s\text{-}h})^n \phi(s)\, d_s \tag{11}$$

If the two rough surfaces are in consideration, then β and σ are to be modified as given in Eq. (12) and Eq. (13) respectively.

$$\beta = \frac{\beta_1\beta_2}{\beta_1 + \beta_2} \tag{12}$$

$$\sigma = \sqrt{\sigma_1^2 + \sigma_2^2} \tag{13}$$

The subscripts 1 and 2 refer to the two contact rough surfaces. Hamilton and Goodman [17] suggested that the two principal stresses are largely compressive in nature. The third principle stress is of tensile nature and it is this principle stress that is mainly responsible for the generation of crack and leads to fatigue failure. So they derived the equation for tensile stress for the fatigue failure Eq. (14).

$$S = \frac{3P_1}{2\pi a_1^2}\left(\frac{\mu}{8}(4+\gamma)\pi + \frac{(1-2\gamma)}{3}\right) \tag{14}$$

where S is tensile stress, γ is Poisson's ratio, μ is friction coefficient, P_1 is Load and a_1 is contact radius. The P_1 and a_1 could be determined from Eq. (15-16) provided that the average size of each micro contact is nearly constant for elastic contact situation [18].

$$P_1 = \frac{P}{\eta A_0 F_0(h)} \tag{15}$$

$$a_1 = \sqrt{\frac{\beta\sigma F_1(h)}{F_0(h)}} \tag{16}$$

Substituting these two values in Eq. (14) then the expression of tensile stress is given by Eq. (17)

$$S = \frac{3k_1 P}{2\pi\eta A_0 \beta\sigma F_1(h)} \tag{17}$$

where

$$k_1 = \frac{\mu}{8}(4+\gamma)\pi + \left(\frac{1-2\gamma}{3}\right) \tag{18}$$

To determine the failure in an asperity, the bulk fatigue property of material was represented by Wohler's curve, presented in Eq. (19) [19].

$$N_f = \left(\frac{S_0}{S}\right)^t \tag{19}$$

where, N_f is number of cycles to failure, S_0 is failure stress, S is applied cyclic stress and t is material constant. To find the number of cycles for which failure occurs is given as Eq. (20).

$$N_f = \left(\frac{2\pi S_0 \eta A_0 \beta\sigma F_1(h)}{3k_1 P}\right)^t \tag{20}$$

The wear work rate $\mathrm{V_R}$ and wear volume V is summarized as Eq. (21) and Eq. (22) respectively.

$$V_R = \frac{\eta_l V_p \mu F_0(h)(k_1 P)^t (A_0\eta)^{1-t}}{\left[\left(\frac{2\pi}{3}\right) S_0 \beta\sigma F_1(h)\right]^t} \tag{21}$$

$$V = \frac{k_1 P L \eta_L v_p}{2S_o}\left(\mu\left(\frac{4+\gamma}{8}\right)\pi + \left(\frac{1-2\gamma}{3}\right)\right) \tag{22}$$

where

$$k_1 = \left[\left(\frac{2k_1 E'}{\pi S_0}\right)^{t-1}\left(\frac{1}{\beta}\right)^{\left(\frac{1+t}{2}\right)}\sigma^{\left(\frac{t-3}{2}\right)} \left(\frac{F_{\frac{3}{2}}(h)}{F_1(h)}\right)^{t-1}\left(\frac{F_0(h)}{F_1(h)}\right)\right] \tag{23}$$

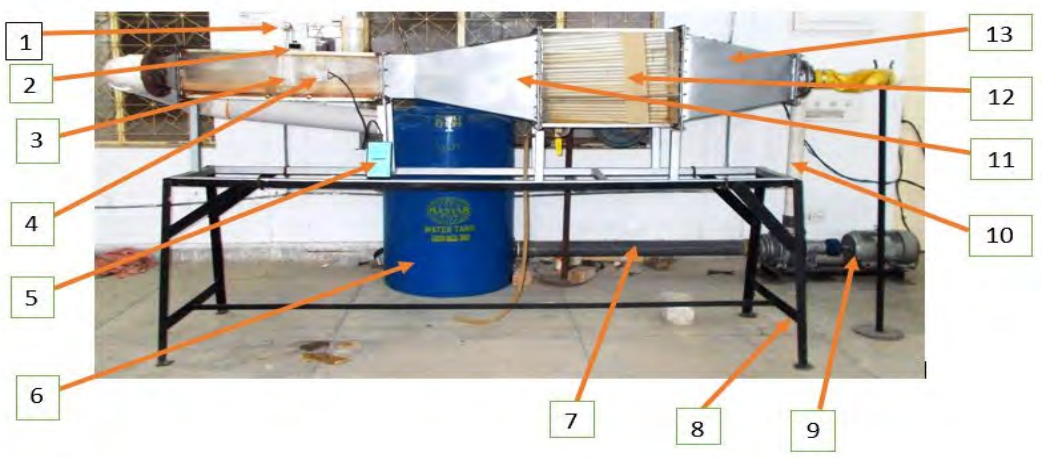

FIGURE 1. Photograph of experimental setup (1) Tube bundle (2) G-Link Tri-Axial accelerometer (3) Test section (4) Flow meter transducer (5) Doppler flow meter (6) Water tank (7) Pump suction line (8) Water tunnel stand (9) 10 HP Motor with centrifugal pump (10) Pump delivery line (11) Convergent section (12) Flow straightener section (13) Divergent section.

The model proposed by Lin and Cheng [20] is the dynamic wear model. This model holds in it the dynamic aspect of the wear process. The basic equation of this model is given as Eq. (24).

$$W_R = \frac{KF}{U} \tag{24}$$

where F is forcing term induced by sharing of asperities, U is wear resistance of the material, W_R is wear volume/unit sliding distance and K is dimensionless constant. For the rough surface, the shear force F is expressed by an average shear force on all the asperities in the possible contact area. Mathematically it can be expressed as Eq. (25). The wear resistance U can be represented as Eq. (26).

$$F = \frac{A_0}{h}\int_0^h \phi_i(z)\,\tau_{i\,avg}(z)dz \tag{25}$$

$$U = \frac{1}{A_0 h}\int_0^h \iint \delta_i(x,y,z)\,d_x d_y d_z \tag{26}$$

where A_0 is normal area, h is asperity height, $\phi_i(z)$ is proportional function of asperity height distribution and $\delta_i(x, y, z)$ is flow strength to assist elasticity or plasticity. The model can be reduced to Achard model where adhesive wear is under account [20]. Also, the published data suggests that this model is very suitable for non linear wear behavior. Magel [21] originally formulated this model to accounts for wear produced by sliding a hard sphere on a flat surface. But later, after experimentation and simulations, this model was found suitable to be applied on a heat exchanger tube bundle. The model is based on the principle that when a relatively hard surface is pressured against a soft surface, the contact pressures may exceed the elastic yield point and plastic deformation will commence. As the cycle goes on, the geometry of the surface starts resembling just like indenter marking on the surface. If the pressurre beneath the spherical surface (like indenter) does not increase the shakedown pressure p_o^s, the material deformation stops. The total force applied by the indents on the surface is given as Eq. (27).

$$P(x) = \pi p_o^s ab \tag{27}$$

As the contact between the indenter and soft surface is considered to be line contact so,by Hertzian contact theory expressed in the form Eq. (28-31).

$$a = 2\sqrt{\frac{P' R_L}{\pi E'}} \tag{28}$$

$$P_0 = \sqrt{\frac{P' E'}{\pi R_L}} \tag{29}$$

$$E' = \frac{1}{\left(\frac{1-\gamma_1^2}{E_1} + \frac{1-\gamma_2^2}{E_2}\right)} \tag{30}$$

$$R_L = \frac{1}{\left(\frac{1}{r_L} - \frac{1}{\rho}\right)} \tag{31}$$

where, P' is load/length, ρ is longitudinal curvature and R_L is radius of indenter. By using the above Eq.(28-31), the Magel [21] derived the final equation of total force of indenter.

$$p(x) = \frac{2\pi l \left(P_0^s\right)^2}{E'}\sqrt{\frac{r_T}{\rho}}\left(\frac{1}{r_L} - \frac{1}{\rho}\right)^{-1}\sqrt{1 - \frac{x^2}{l^2}} \tag{32}$$

Magel extended his model to non-smooth surfaces in sliding [21]. According to his experimental results, the single indentation geometry is well presented using this model. But multi-asperity model overestimates the wear volumes.

In summary, a number of models have been proposed to estimate the wear produced on metal surfaces with different operating conditions. Although the nature of wear due to tube-baffle interaction is quite similar to other metal-metal

FIGURE 2. Flow control mechanism (1) Testing rig (2) Valve 1 (3) Valve 2 (4) water tank.

wear, experimentation is required more often to understand the complete wear phenomenon. Because of this, the current study focuses on the experimental study of the wear produced due to vibration interaction between the tube and baffle plate at different velocities and interaction spans.

III. EXPERIMENTAL SETUP

Experimentation has been completed on the low speed closed channel water tunnel with the range of speed from 0.18 to 0.55 m/s in the test section. The tunnel was designed and developed by Flow-Induced Vibrations Research Group (FIVRG) at University of Engineering and Technology Taxila. The test section of the rig is made up of acrylic plates and the material used for converging and diverging part is metallic. The experimental setup has been presented in Fig. 1.

The test section has dimensions of 200 mm × 100 mm and is made up of acrylic plates that are screwed together. A 10 HP centrifugal pump and 200 gallons water tank is used to maintain the closed loop water flow. The main valve (Valve 1) and bypass (Valve 2) are given to control water speed in the test section up to its maximum value of 0.55 m/s with each increment of 0.09 m/s Fig. 2. An ultrasonic flow meter (Doppler type) was mounted in the test section to measure the upstream speed of the water. Because of its working nature, the flow measuring transducer was mounted on the external surface of the test section. Water is drawn from the water tank, accelerated and passed through the test section. The deliberately structured flow straightener guarantees a uniform speed distribution with the intensity of turbulence less than 3%. The tube bundle under investigation was mounted in the test section while the flow medium water was set in motion, thus the desired flow around the tubes in a tube bundle was generated. The drawing and picture of tube bundle have been presented in Fig. 3.

To monitor the vibrations in stream-wise (Y, in the direction of flow) and transverse (X, perpendicular to flow) direction the wireless tri-axial accelerometer was mounted on the monitored tube. The monitored tube is suspended with the help of piano wire of 0.2mm thickness with the tensioning mechanism provided to adjust the natural frequency of the monitored tube. The natural frequency of the monitored tube was tuned to 8±0.1 Hz. In order to capture the vibration response of the monitored tube in crossflow, the accelerometer was mounted on the top of the monitored tube. Two acrylic plates were used to support the whole assembly while one of them was used to hold the rigid tubes and the other used to hold the tensioning mechanism Fig. 4(a). Table 1 presents the tube bundle specifications.

The tests were performed on five different flow velocities with each increment of 0.09 m/s. For each flow velocity, tests were performed for three-time spans i.e. 30 minutes, 60 minutes and 90 minutes. A total of 15 sets of experiments had been conducted. A Scanning Electron Microscope (SEM) was used to analyze and measure the size of wear scars created on the tubular surface during experimentation Fig. 5.

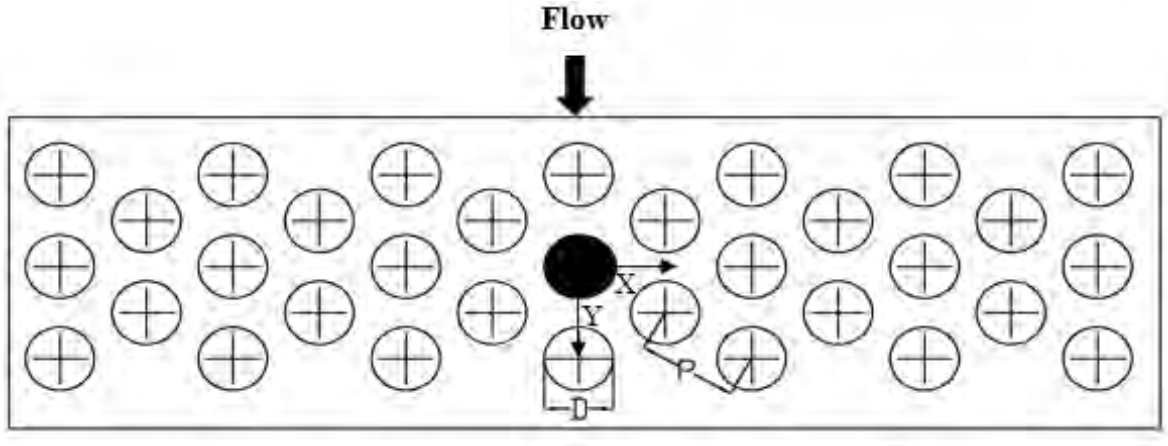

FIGURE 3. Drawing of the tube bundle with P/D of 1.45 (X = Transverse, Y = stream-wise).

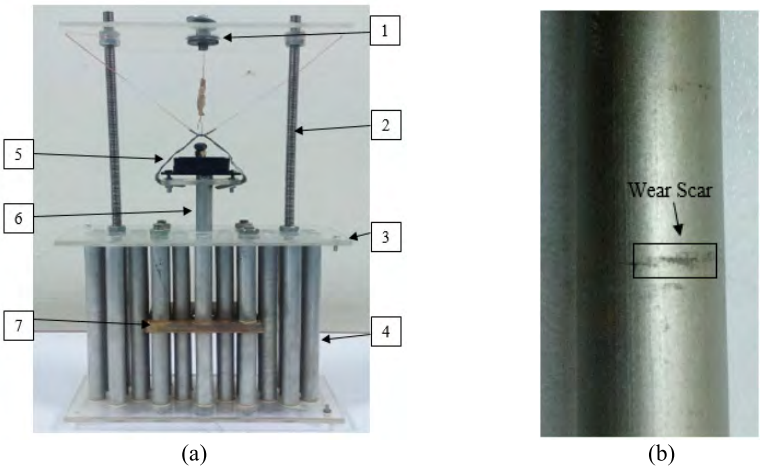

FIGURE 4. (a) Photograph of tube bundle (1) Tensioning mechanism (2) support stud (3) support plates (4) Rigid tubes (5) Accelerometer (6) Monitored tube (7) Baffle (b) Photograph of tube indicating wear scar.

TABLE 1. Specification of the tube bundle.

Tube material	Aluminum
Tube arrangement	Parallel triangular
Mass of the tube	0.072 kg
P/D ratio	1.45
Tube outer/inner diameter	12.7 mm/ 11.5 mm
Tube length	228 mm
Modulus of Elasticity	69000 MPa
Density of water	1000 kg/m^3
Baffle thickness	0.6 mm
Baffle hole diameter	15 mm
Tube to baffle radial clearance	1.15 mm

FIGURE 5. Photograph of scanning electron microscope (SEM).

The monitored tube was removed from the tube bundle and a total of 15 samples were prepared for three different time spans (30 minutes, 60 minutes and 90 minutes) and five different velocities for measurement of length and width of wear scar in SEM. A new technique was used to measure the depth. Cross surface profiles of various samples of known wear depth on similar tube material were captured by using SEM. A calibration curve was plotted on the base of these measurements. A conversion factor was deduced from the calibration curve i.e. (1 Adu $=$ 0.3055 μm). The wear depth of wear scars formed in the experiments was estimated on the base of the conversion factor. The complete analysis has been discussed in section IV.

IV. EXPERIMENTAL RESULTS AND DISCUSSIONS

A. VIBRATION ANALYSIS

Fig. 6 presents the vibration signals of the stream-wise and transverse direction of the tube for a velocity of 0.18 m/s (lowest) Fig. 6(a, b) and 0.55 m/s (highest) Fig. 6(c, d) and Fig. 7 presents the RMS amplitude response of the tube with an increase in the crossflow velocity.

It can be seen that at a velocity of 0.18 m/s, the tube vibrates with the smaller amplitude as compared to transverse amplitude which is slightly higher Fig. 6(a, b).This difference between amplitudes in both directions is significant at a velocity of 0.55 m/s with a transverse amplitude about 5 times that of stream-wise amplitude Fig. 6(c, d). The Fig. 7 shows a more elaborated view of the tube response. It can be seen that the stream-wise amplitude shows a small rise in amplitude as the cross-flow velocity increases, however, for the transverse direction the amplitude rises significantly after the velocity of 0.27 m/s and continues to rise with the cross-flow velocity and reaches a maximum RMS amplitude of about 5 m/s^2 at the maximum velocity.

Although at first, it seems that the transverse amplitude value represents the magnitude of tube vibration but in fact, it may be due to impacting of the tube with the inner surface of the baffle hole. This results in significant wear produced at high velocities and predominantly in the transverse direction.

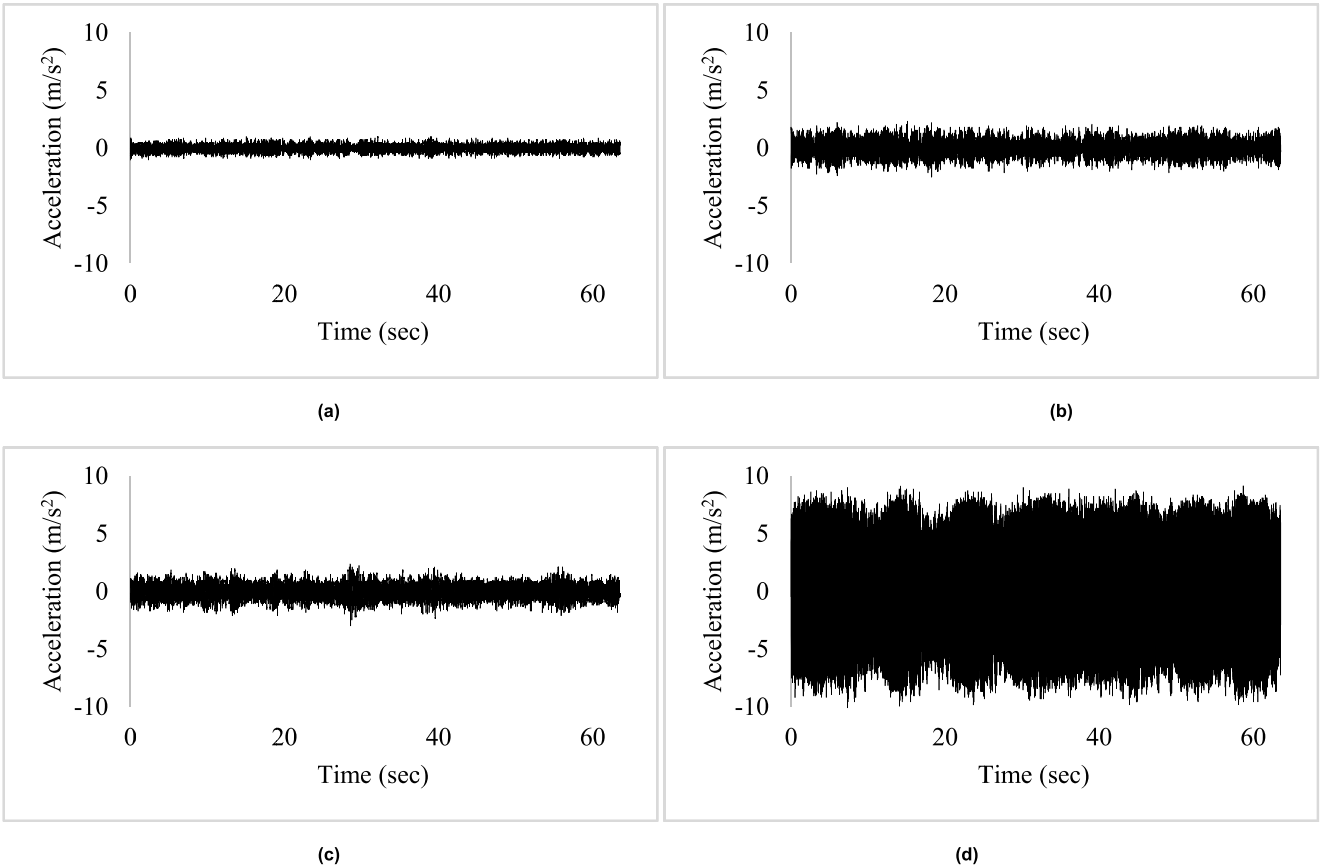

FIGURE 6. Vibration signals of the tube (a) Stream-wise (Velocity = 0.18 m/s); (b) Transverse (Velocity = 0.18 m/s); (c) Stream-wise (Velocity = 0.55 m/s); (d) Transverse (Velocity = 0.55 m/s).

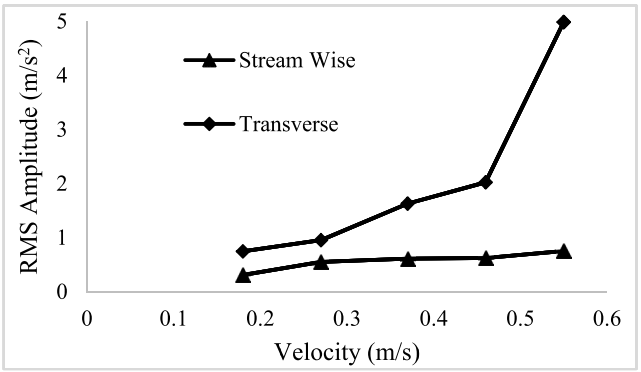

FIGURE 7. RMS amplitude response of the monitored tube in cross-flow.

So the acceleration amplitude seems to have a strong relationship with the wear produced in the tube, which has been further discussed in the later sections.

B. SCANNING ELECTRON MICROSCOPE (SEM) IMAGES AND WEAR PROFILES

The scanning electron microscope (SEM) images and the wear profiles of the tube for different durations at the maximum velocity of 0.55 m/s have been presented in Fig. 8. The analysis of the wear profiles and the corresponding wear characteristics suggest that the wear width tends to increase with the time span between the tube and the baffle. Also, the wear depth tends to follow the same pattern.

It can be observed in wear profiles, there are relatively small profile peaks visible for the duration of 30 minutes and 60 minutes Fig. 8(a, b). This corresponds to a relatively small wear depth. But for 90 minutes duration, a sharp profile with relatively higher peaks can be seen that indicates the high wear depth Fig. 8(c).

C. INVESTIGATION OF THE WEAR SIZES

1) WEAR LENGTH

The variation of wear length has been presented in Fig. 9. It can be seen that the wear length increases gradually with the increase in the cross-flow velocity. For the 30 minutes of interaction between the tube and baffle, the wear length was around $0.4\times10^3\mu$m at a velocity of 0.18 m/s and 0.27 m/s. However, a significant rise has been observed when the velocity was increased beyond 0.27 m/s with maximum wear length reaching to about $0.96\times10^3\mu$m. This trend has also been observed for the other two time spans i.e. 60 minutes and 90 minutes, except the maximum wear length for 60 minutes

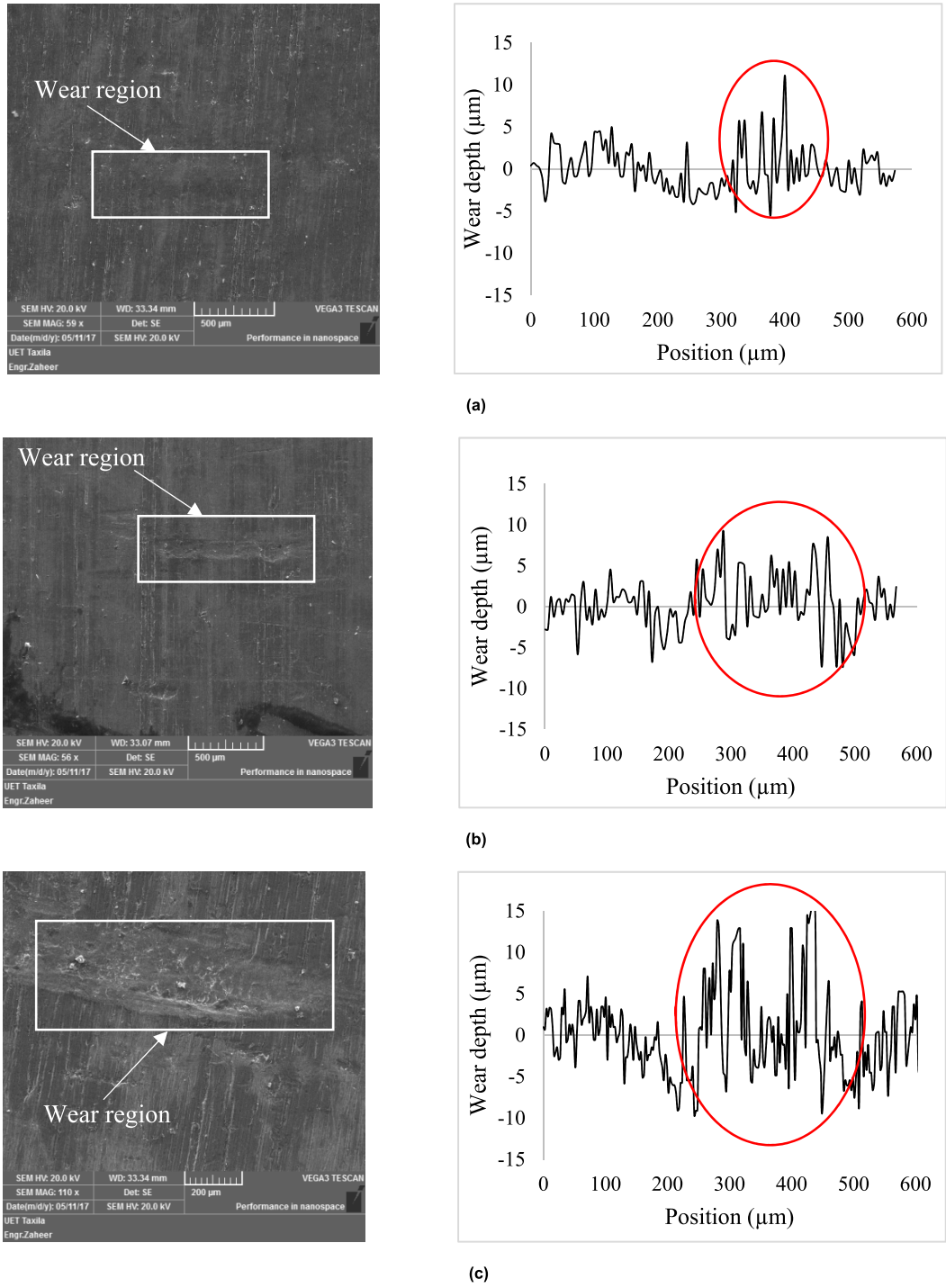

FIGURE 8. Scanning electron microscope (SEM) images and cross wear profiles of the tube at a velocity of 0.55 m/s for (a) 30 minutes (b) 60 minutes (c) 90 minutes.

time span is about $1.1 \times 10^3 \mu$m and $1.26 \times 10^3 \mu$m for a time span of 90 minutes.

It is also very important to note that the slope of the trend line seems to be increasing as the time span increases. The slope determined based on the trend line is 1618 (μm/ms^{-1}) for 30 minutes time span, 1834 (μm/ms^{-1}) for 60 minutes and 3010 (μm/ms^{-1}) for 90 minutes. The difference in the slope of the trend lines suggests that the wear length tends to increase significantly as the time span increases.

2) WEAR AREA

Fig. 10 presents the variation of wear area with the increase in the velocity for all three durations. The wear area has been

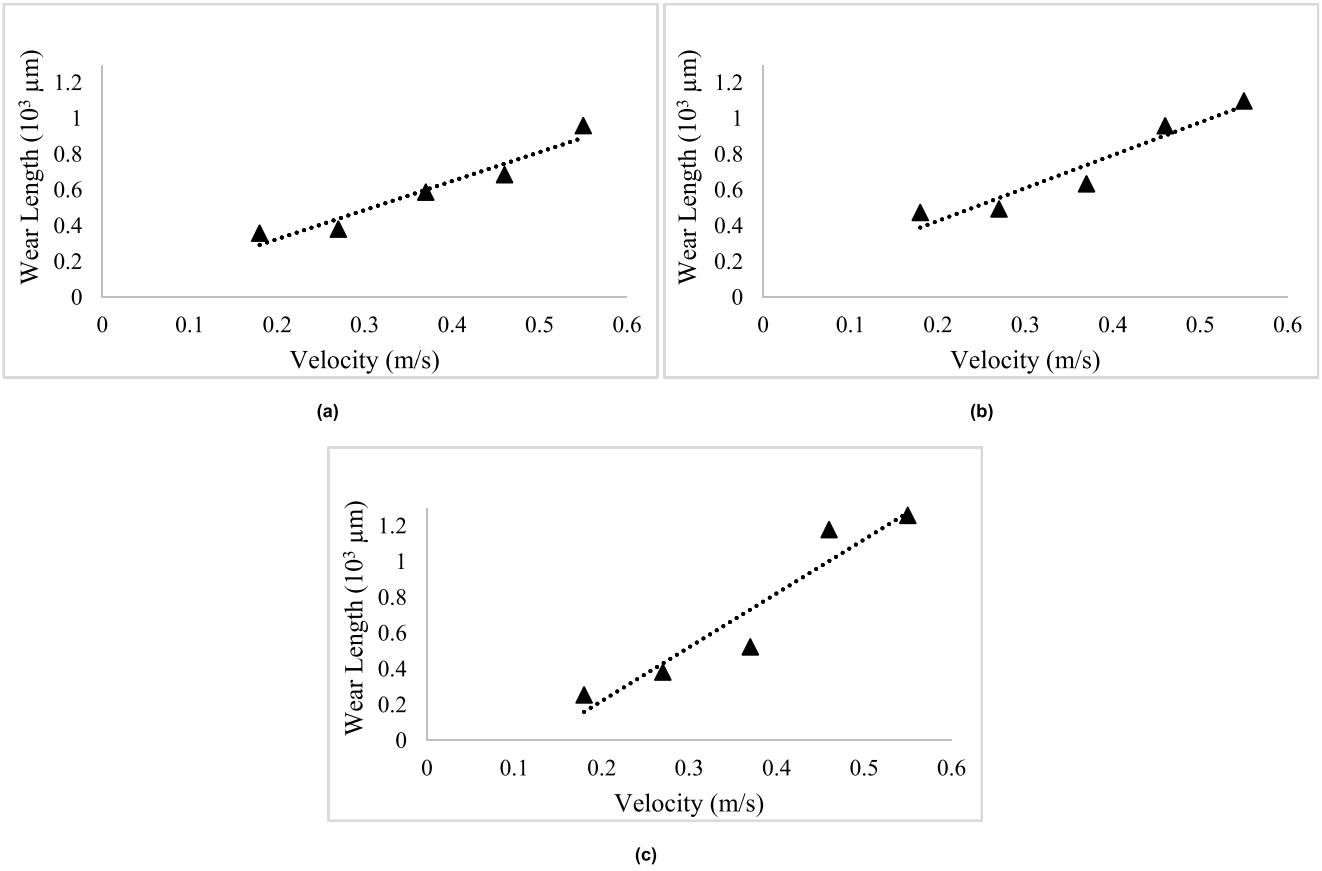

FIGURE 9. Variation of Wear length with cross flow velocity for (a) 30 minutes (b) 60 minutes (c) 90 minutes.

calculated from the wear length and width. As it can be seen that there is no significant difference in the wear area for all three durations up to cross-flow velocity of 0.37 m/s justified by the small amplitudes of vibration and thus less tendency of the interaction between the tube and the baffle. However, when the velocity crosses the value of 0.37 m/s, the wear area tends to increase significantly with an increase in the cross-flow velocity. Also, it is very important to note that beyond the velocity of 0.37 m/s, the trend of wear area is distinct for each duration. When the monitored tube reaches near the stability threshold related to fluidelastic instability (as in the case of 0.37 m/s), the vibration orbit of the tube tends to shift from random to organized elliptical orbits with the major axis aligned along the transverse direction. Due to this behavior, the contact time as well as contact area between the tube and baffle tends to increase significantly. As a result, there is also a significant rise in wear width apart from the wear length and in turn increase in the wear area even before the stability threshold.

In fact, a maximum value of about 170×10^{-3} mm^2 of wear area has been observed for the maximum duration (90 minutes) and a minimum value of about 130×10^{-3} mm^2 for 30 minutes duration.

3) WEAR VOLUME

Based on the estimation of the depth from the analysis of wear scars from the scanning electron microscope (SEM) images, a wear volume analysis has been carried out to investigate its relationship with the three different durations and five different velocities. Fig. 11 and Fig. 12 presents the trend of wear volume of the tube for different durations and velocities respectively.

The analysis suggests that the wear volume shows an increasing trend with the increase in the velocity. For the duration of 30 and 60 minutes, there is no significant difference in the behavior of the wear volume even at high velocities with the maximum value approaching about 1×10^{-3} mm^3, but for the 90 minutes duration the behavior tends to be distinct and shows a significant rise in the wear volume which is about 35% larger as compared to the other two durations as presented in Fig. 11. The analysis also suggests that at the maximum velocity of 0.55 m/s even at 30 minutes duration there is a relatively higher value of wear volume which otherwise is very small for lower velocities. Based on the current analysis a linear trend cannot be expected between the wear volume and the time span between the tube and baffle. A comprehensive study is required which should include the

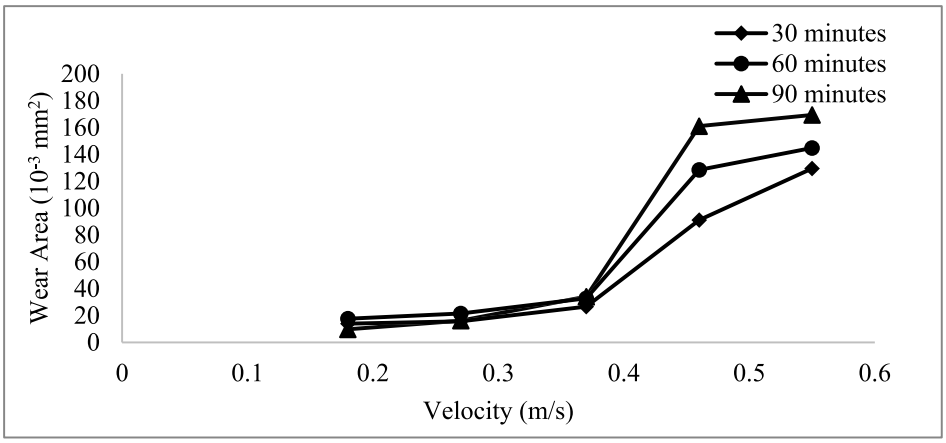

FIGURE 10. Wear area of the tube with an increase in velocity.

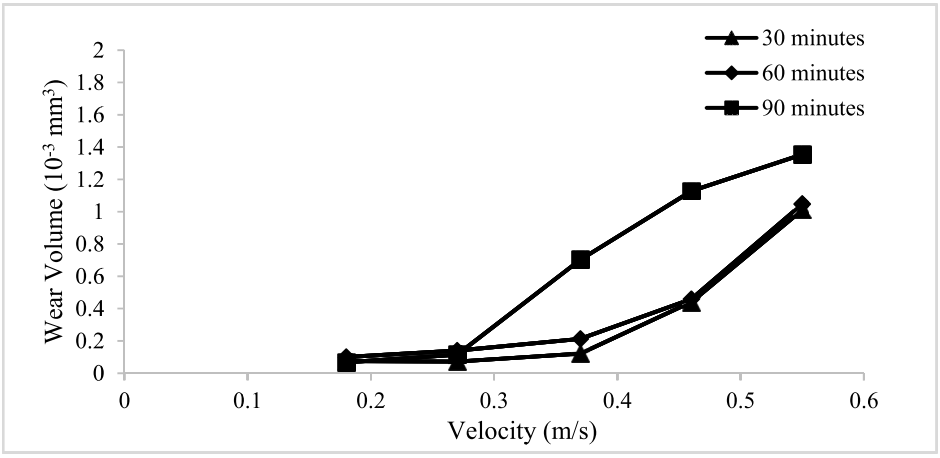

FIGURE 11. Wear volume of the tube for different durations.

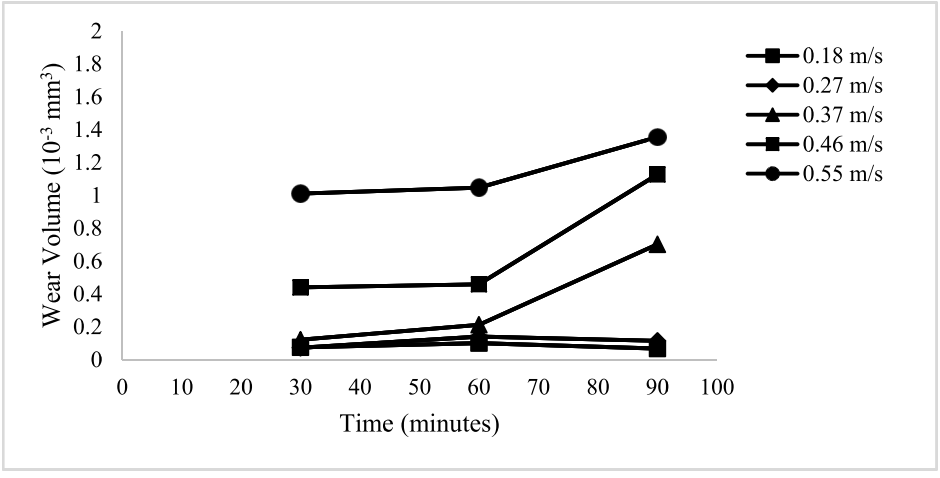

FIGURE 12. Wear volume of the tube for different velocities.

wear analysis for long durations in order to confirm this wear behavior of the tubes.

A comparison has been presented between the parameters of the current experiment and the experiment conducted by Kim et al. [6] Table 2. They presented a relationship between the wear area and the wear volume for the nuclear fuel rod with different conditions. The trend between the wear area and wear volume is also presented for both experiments (current and Kim et al.) Fig. 13.

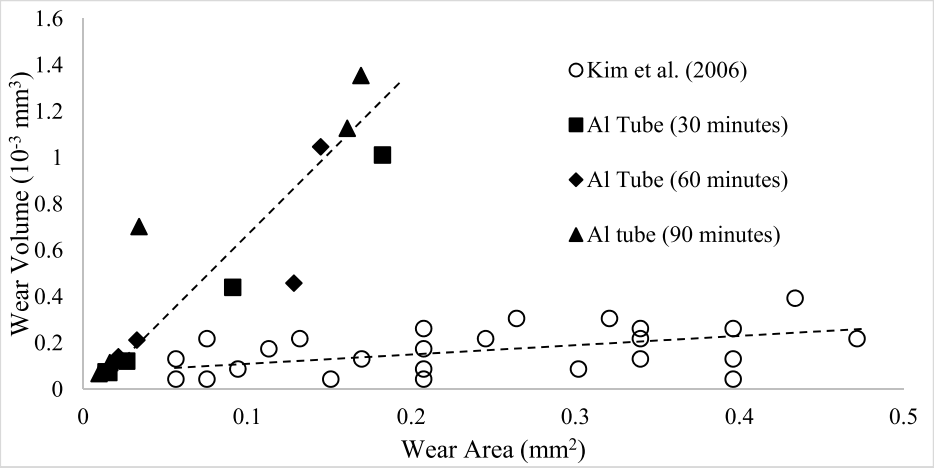

FIGURE 13. Relationship between wear volume and wear area.

TABLE 2. Comparison of mechanical properties.

	Current Experiment	H. K. Kim et al. [6]
Material	Aluminum	Zircaloy-4
Mechanical properties		
Tensile strength	310 MPa	470 MPa
Yield strength	240 MPa	315 MPa
Elastic Modulus	69 GPa	136.6 GPa
Poisson's Ratio	0.32	0.294

The trend for the aluminum tube for low wear area seems to be very similar to a nuclear fuel rod but as the wear area increases, there is more acceleration in the wear volume for the aluminum tube as compared to nuclear fuel rod. This may be due to the material properties of the specimen itself Table 2.

Aluminum is relatively softer thus has a high wear acceleration, whereas a nuclear fuel rod (Zircaloy-4) is generally very hard, that is why there is no accelerated rise in the wear depth which is actually confirmed by the current comparison. From the current comparison, the slope of the trend line also shows the rate of wear produced in both the specimens.

V. CONCLUSION

From the current study the following conclusion can be made:

The transverse direction amplitude rises significantly after the velocity of 0.27 m/s and continues to rise in the cross-flow velocity at the maximum velocity of 0.55 m/s. Significant wear has been produced at higher velocities predominantly in the transverse direction. Wear length increases gradually with the increase in the cross-flow velocity but has a distinct pattern for each time span. The slope of the trend lines for wear length variation increases as the duration of interaction between the tube and baffle hole increases.

Analysis on wear area suggests that there is no significant difference in the wear area for all three durations up to cross-flow velocity of 0.37 m/s, but when the velocity crosses this value the wear area tends to increase significantly with the increase in the cross-flow velocity. For the duration of 30 and 60 minutes, there is no significant difference in the behavior of wear volume even at high velocity, but for the 90 minutes duration, the behavior tends to be distinct and shows a significant rise in the wear volume.

ACKNOWLEDGMENT

The authors gratefully acknowledge the financial and technical support of the University of Engineering and Technology Taxila (UET, Taxila) and Higher Education Commission (HEC) Pakistan.

REFERENCES

[1] H.-K. Kim and Y.-H. Lee, "Influence of contact shape and supporting condition on tube fretting wear," *Wear*, vol. 255, pp. 1183–1197, Aug./Sep. 2003.
[2] P. L. Ko, "Metallic wear—A review with special references to vibration-induced wear in power plant components," *Tribology Int.*, vol. 20, pp. 66–78, Apr. 1987.
[3] H. C. Meng and K. C. Ludema, "Wear models and predictive equations: Their form and content," *Wear*, vol. 181, pp. 443–457, Mar. 1995.
[4] N. J. Fisher, A. B. Chow, and M. K. Weckwerth, "Experimental fretting-wear studies of steam generator materials," *J. Pressure Vessel Technol.*, vol. 117, no. 4, pp. 312–320, 1995.
[5] T. Joulin, F. M. Guérout, A. Lina, and D. Moinereau, "Effects of loading conditions and types of motion on PWR fuel rod cladding wear," in *Proc. ASME Int. Mech. Eng. Congr. Expo.*, 2002, pp. 1011–1018.
[6] H.-K. Kim, Y.-H. Lee, and S.-P. Heo, "Mechanical and experimental investigation on nuclear fuel fretting," *Tribology Int.*, vol. 39, pp. 1305–1319, Oct. 2006.
[7] H. J. Connors, "Flow-induced vibration and wear of steam generator tubes," *Nucl. Technol.*, vol. 55, no. 2, pp. 311–331, 1981.

[8] R. D. Blevins, "Fretting wear of heat exchanger tubes," General Atomics, San Diego, CA, USA, Tech. Rep. GA-A-14817; CONF-780922-1, 1978.
[9] P. L. Ko, "Heat exchanger tube fretting wear: Review and application to design," *J. Tribology*, vol. 107, pp. 149–156, Apr. 1985.
[10] M. Au-Yang, "Flow-induced wear in steam generator tubes: Prediction versus operational experience," *ASME-PUBLICATIONS-AD*, vol. 53, pp. 265–274, 1997.
[11] M. Yetisir, E. McKerrow, and M. J. Pettigrew, "Fretting wear damage of heat exchanger tubes: A proposed damage criterion based on tube vibration response," *J. Pressure Vessel Technol.*, vol. 120, pp. 297–305, Aug. 1998.
[12] S. Khushnood, Z. M. Khan, M. A. Malik, Z. Koreshi, and M. A. Khan, "Modeling and simulation of cross-flow induced vibration in a multi-span tube bundle," in *Proc. 12th Int. Conf. Nucl. Eng. (ICONE)*, Arlington, VA, USA, 2004, pp. 253–264.
[13] J. F. Archard, "Contact and rubbing of flat surfaces," *J. Appl. Phys.*, vol. 24, no. 8, pp. 981–988, 1953.
[14] K.-W. Ryu, C.-Y. Park, H.-N. Kim, and H. Rhee, "Prediction of fretting wear depth for steam generator tubes based on various types of wear scars," *J. Nucl. Sci. Technol.*, vol. 47, no. 5, pp. 449–456, 2010.
[15] V. K. Jain and S. Bahadur, "Experimental verification of a fatigue wear equation," *Wear*, vol. 79, pp. 241–253, Jul. 1982.
[16] J. A. Greenwood and J. B. P. Williamson, "Contact of nominally flat surfaces," *Proc. Roy. Soc. London A, Math., Phys. Eng. Sci.*, vol. 295, pp. 300–319, Dec. 1966.
[17] L. E. Goodman and G. M. Hamilton, "The stress field created by a circular sliding contact," *J. Appl. Mech.*, vol. 33, no. 2, pp. 371–376, 1966.
[18] J. A. Greenwood, "The area of contact between rough surfaces and flats," *J. Lubrication Technol.*, vol. 89, no. 1, pp. 81–87, 1967.
[19] M. M. Reznikovskii, "Relation between the abrasion resistance and other mechanical properties of rubber," in *Abrasion of Rubber*. London, U.K.: Maclaren, 1967, pp. 119–126.
[20] J.-Y. Lin and H. S. Cheng, "An analytical model for dynamic wear," *J. Tribology*, vol. 111, no. 3, pp. 468–474, 1989.
[21] E. E. Magel, "Experimental and theoretical studies of the wear of heat exchanger tubes," Univ. British Columbia, Vancouver, BC, Canada, 1990.

MUHAMMAD USMAN received the bachelor's in mechanical engineering from the University of Lahore, Lahore, Pakistan, and the master's degree in mechanical engineering from the University of Engineering and Technology, Taxila, Pakistan. He is currently serving as a Lecturer in the Mechanical Engineering Department, The University of Lahore, Lahore, Pakistan.

His research interest includes flow induced vibrational analysis of tube wear in cross flow in tube bundles in heat exchangers.

SHAHAB KHUSHNOOD received the bachelor's and master's degree in mechanical engineering from The University of Engineering and Technology, Lahore, Pakistan, and the Ph.D. degree from the National University of Science and Technology, Rawalpindi, Pakistan, in 2005. He served as the Dean for the Faculty of Mechanical and Aeronautical Engineering, University of Engineering and Technology, Taxila.

His research interests include vibration analysis of shell and tube heat exchanger, heat transfer analysis in heat exchangers, and optimization.

LUQMAN AHMAD NIZAM received the bachelor's and master's degree in mechanical engineering from the University of Engineering and Technology, Taxila, Pakistan, where he is currently pursuing the Ph.D. degree. He is currently serving as an Assistant Professor in the Mechanical Engineering Department, HITEC University, Taxila Cantt, Pakistan. His research interests include vibration analysis of tube bundles and optimization.

MUHAMMAD AYUB received the bachelor's degree in mechanical engineering from The University of Lahore, Lahore, Pakistan, and he is pursuing the master's degree in mechanical engineering from International Islamic University, Islamabad, Pakistan.He is currently serving as a Laboratory Engineer in the Mechanical Engineering Department, The University of Lahore, Lahore, Pakistan.

His research interest includes parametric analysis of fretting wear of flexible tube in heat exchanger.

AKMAL HAFEEZ received the bachelor's degree in mechanical engineering from the University of Lahore, Lahore, Pakistan and is currently pursuing the master's degree in mechanical engineering from the University of Engineering and Technology, Taxila.

His research interest includes FIV analysis of glass tubes in cross flow.

BEHZAD RUSTAM received the bachelor's and Master's degree in mechanical engineering from The University of Lahore, Lahore, Pakistan. He is serving as an Assistant Professor in the Mechanical Engineering Department, The University of Lahore, Lahore, Pakistan.

His research interest includes analysis of within the desiccant and without the desiccant dehumidification system performance.

JUNAID MUHAMMAD YOUSUF received the bachelor's degree in mechanical engineering from the University of Lahore, Lahore, Pakistan, where he has been a Laboratory Engineer with the Department of Mechanical Engineering.

His research interest includes fluid-object interaction, thermodynamics, and experimentation design.

MUHAMMAD SHAHID BASHIR received the bachelor's degree in mechanical engineering from the University of Engineering and Technology, Lahore, Pakistan and is pursuing the M.S. degree in mechanical engineering from the University of Engineering and Technology, Taxila.

His research interest includes experimental wear analysis of flexible tube with varying support plate geometry.